Observation of axisymmetric dark plasma excitations in a two-dimensional electron system

V. M. Muravev, I. V. Andreev, V. N. Belyanin, S. I. Gubarev, and I. V. Kukushkin
Institute of Solid State Physics RAS, Chernogolovka 142432, Russia
(Received 4 April 2017; published 17 July 2017)

Resonant microwave absorption of two-dimensional electron systems in AlGaAs/GaAs heterostructures with a single Corbino disk geometry has been studied. Axisymmetric dark plasmon modes have been excited using a near-field excitation technique, and their magnetodispersion have been determined in the presence of a perpendicular magnetic field. Plasma excitations observed have been compared to bright plasmon modes in a single disk of identical geometry. Dark plasmon modes have been found to have considerably longer lifetimes compared to bright plasmon modes due to the inhibition of superradiant losses.

DOI: 10.1103/PhysRevB.96.045421

Research on plasma excitations in two-dimensional electron systems (2DESs) has experienced a renaissance in recent years [1]. This interest has partly been fueled by the promise of possible applications in the field of detection and generation of terahertz radiation [2–5]. Plasma waves in the 2DESs can be reduced to dark and bright modes as the two elementary building blocks [6]. In the ultimate two-dimensional (2D) disk geometry plasmons are classified by a set of two integer numbers, $(m;l)$ [7], where $m = 0,\pm1,\pm2...$, is an azimuthal index, and $l = 1,2,3...$ is a radial index. Bright modes with $m \neq 0$ sustain dipolar and multipolar plasmon excitations with a specific number of field antinodes along the disk circumference, and are normally observed in all experiments [8]. In a zero magnetic field the spectrum of two-dimensional (2D) plasmons follows the standard square-root dispersion law [7,9]:

$$\omega_p^2(q) = \frac{n_s e^2}{2m^*\varepsilon_0\varepsilon} q, \tag{1}$$

where n_s and m^* are density and effective mass of 2D electrons, while ε_0 and $\varepsilon = (\varepsilon_{\mathrm{GaAs}} + 1)/2$ are vacuum permittivity and effective permittivity of the surrounding medium, respectively. The fundamental bright plasma excitation $(m = \pm1, l = 1)$ possess the wave vector q determined by the disk circumference $q \approx 2\pi/\lambda = 2\pi/\pi D = 2/D$ [7,10].

Dark modes with $m = 0$ have an axisymmetric distribution of the electric potential and are similar to the vibrations of a circular membrane. The fundamental dark plasma excitation $(m = 0, l = 1)$ wave vector q is scaled by the disk radial confinement $q \approx 2\pi/D$ [7]. These axisymmetric modes have no angular dependence of their electric potential and therefore have a zero net dipole moment. Dark plasmon modes, by virtue of their zero dipole moments, exhibit suppressed superradiant losses, and consequently a high Q factor and large propagation lengths. Despite their very peculiar symmetry and physical properties, axisymmetric plasmon modes in 2DESs have not been observed so far in solid-state systems and have not been properly studied [11,12]. This is partially due to the fact that axisymmetric dark plasma waves cannot be excited by linearly polarized incident electromagnetic waves, and special techniques have to be used for their excitation.

In this work, we developed a special technique to excite axisymmetric plasma modes in a Corbino geometry. The 2DESs samples used for our investigation had a disk geometry of diameter D with a grounded ohmic contact on the perimeter of the disk, and a concentric circular conductive gate of considerably smaller diameter, $d \ll D$, which was fabricated at the disk center [Fig. 1(b), inset]. This Corbino sample geometry met the requirement of axial potential symmetry, necessary for the excitation of the $m = 0$ dark plasmon mode. The microwave radiation with frequencies from 2 to 50 GHz was guided into the cryostat with a coaxial cable, and transferred to the excitation gate via an impedance-matched coplanar waveguide transmission line. Our samples were fabricated from high-quality modulation-doped GaAs/AlGaAs heterostructures, with a quantum well with a width of 25 nm. The electron density of the 2DES was $n_s = 1.0 \times 10^{11}\mathrm{cm}^{-2}$, and the electron mobility at $T = 4.2$ K was $5 \times 10^6\mathrm{cm}^2/\mathrm{V\,s}$. The experiments were conducted on a series of samples with diameters $D = 2, 1, 0.5$ mm, and $d = 0.14, 0.1, 0.05$ mm, respectively. The samples were placed in a liquid helium cryostat at the center of a superconducting coil. Our experiments were carried out by applying a magnetic field of 0–0.5 T perpendicular to the sample surface, at a temperature of $T = 1.5$ K. To detect the microwave absorption in the 2DES, we employed a noninvasive optical technique [13,14]. The essence of the technique is that the 2D electron luminescence spectrum is highly sensitive to the 2DES temperature. The luminescence spectra were measured with and without the incident microwave radiation at a fixed microwave frequency. These spectra were obtained with a grating spectrometer (spectral resolution of 0.03 meV) and recorded by a CCD camera. A 0.1-mW continuous-wave laser of wavelength 780 nm was used for the excitation of the 2DES. Next, these spectra were subtracted, and the absolute value of the resulting differential luminescence spectrum integrated across the entire spectrum. The resultant integrated value is a measure of the charge carrier heating under resonant conditions or, identically, a measure of the microwave absorption intensity.

Figure 1(a) shows typical resonant microwave absorption curves as a function of the magnetic field, measured for a sample with dimensions of $D = 500$ μm and $d = 100$ μm, where the horizontal arrow marks the zero level of the microwave absorption intensity. It is evident from the plot that the dependencies derived have a resonant form corresponding to the excitation of a plasma wave, and the resonance shifts towards higher magnetic fields as the microwave frequency f increases. Our experimental results for the magnetodispersion of the plasma excitation observed are plotted in Fig. 1(b) (filled squares). For comparison, the same figure

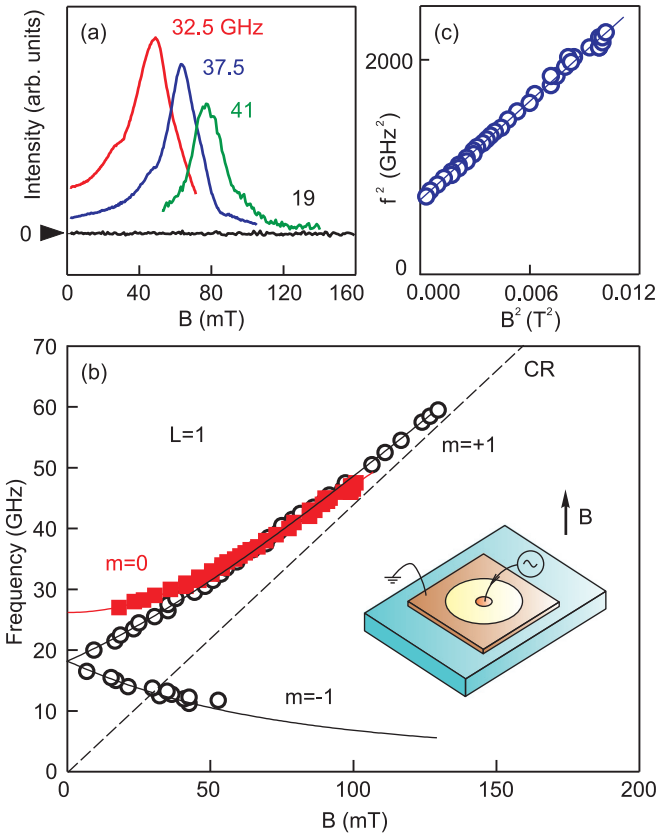

FIG. 1. (a) Microwave absorption intensity in $D = 0.5$ mm size Corbino disk as a function of magnetic field for a series of microwave frequencies f. The electron density is $n_s = 1.0 \times 10^{11}\text{cm}^{-2}$. (b) Magnetodispersion of the axisymmetric dark magnetoplasma mode (squares) and fundamental magnetoplasma mode (circles) observed in a single 2DES disk of the same diameter $D = 0.5$ mm and 2DES density. Axisymmetric magnetoplasma mode ($m = 0$) in the Corbino geometry has only one branch with positive magnetodispersion. (c) Magnetodispersion of the axisymmetric plasmon mode in the $f^2(B^2)$ axes.

shows magnetodispersion of dipole-allowed bright plasma excitations observed in a single 2DES disk with the same diameter of $D = 500$ μm and 2DES density (empty circles), where the plasmons were excited by a plane electromagnetic wave incident on the structure. In contrast to the Corbino geometry, in the bare disk, we observed the fundamental bright plasmon mode, which splits into two branches of a well-known nature in the presence of a perpendicular magnetic field [8]. The high-frequency branch ($m = +1$) has a positive magnetodispersion and corresponds to the excitation of the cyclotron magnetoplasma mode, whose frequency approaches the cyclotron resonance frequency of $\omega_c = eB/m^*$ [Fig. 1(b), dashed line] asymptotically, in the limit of high magnetic fields. Here, $m^* = 0.067m_0$ is the effective electron mass in GaAs. The low-frequency branch ($m = -1$) corresponds to a magnetoplasmon propagating along the edge of the disk. In both cases, the azimuthal index m describes the angular distribution of the induced charge in the plasma wave.

Comparison of the plasmon modes observed in the Corbino and bare disk geometries allows us to identify a number of stark distinctions. (1) The plasmon mode discovered in the Corbino geometry has only a single branch with positive magnetodispersion without corresponding edge magnetoplasma mode. As an example, Fig. 1(a) also shows the magnetic field dependence of the microwave absorption in the Corbino geometry, for the frequency $f = 19$ GHz. We observe that there are no signs of any resonances in the absorption signal. (2) We can also see from Fig. 1(b) that at $B = 0$ T, the resonant plasma frequency of the new mode in the Corbino geometry, $f_0 = 26.4$ GHz, is appreciably larger than the corresponding plasma frequency in the single disk geometry, $f_p = 18.2$ GHz. (3) The behavior of the two modes in the low magnetic field limit is, in fact, entirely different. Indeed, our experimental results for the magnetodispersion of the fundamental bright plasmon mode in a single disk are in good agreement with the theoretical dependence [8,15] [Fig. 1(b), solid lines]:

$$\omega = \pm\frac{\omega_c}{2} + \sqrt{\omega_p^2 + \left(\frac{\omega_c}{2}\right)^2}, \tag{2}$$

and hence, the derivative of the magnetodispersion at zero magnetic field is

$$\left.\frac{\partial\omega}{\partial\omega_c}\right|_{B=0} = \pm\frac{1}{2}.$$

Consequently, there should be a certain angle between the magnetodispersion curve and the B axis at $B = 0$. In contrast, the magnetodispersion of the plasmon mode observed in the quasi-Corbino geometry has a parabolic shape, with its derivative, $\partial\omega/\partial\omega_c$, tending to zero in the low B-field limit, in contrast to the linear shape of (2).

These features are in favor of the dark plasmon nature of the observed mode. Moreover, all the observed distinctive properties of this new mode agree with the theoretical hydrodynamic model built for the axisymmetric ($m = 0$) plasmon mode [7]. As the axial symmetry of the mode presumes no angular dependence of its oscillating charge density, it follows naturally that the edge magnetoplasma branch is not excited in our experiments. It should, however, be noted that in our Corbino geometry, the requirement of a zero angular dependence of the excited plasma modes is provided by the grounded perimetric contact of the 2DES [Fig. 1(b), inset]. Furthermore, theory [7] also predicts that for all axisymmetric modes the squared magnetoplasma frequency necessarily should linearly depend on the squared cyclotron frequency:

$$\omega^2 = \omega_0^2 + \omega_c^2. \tag{3}$$

This common rule was theoretically predicted in a seminal paper [16] for a 2D inversion layer plasma and was later experimentally observed in various low-dimensional systems [17–19]. In Fig. 1(c), the values of the squared magnetoplasma frequency f^2 have been plotted against the squared magnetic field B^2. In accordance with the theoretical prediction, the data fall along a straight line across the entire range of the magnetic field. In addition, the slope of the magnetodispersion curve calculated from (3) in the limit of small magnetic fields, $\partial\omega/\partial\omega_c(B \to 0) = 0$. This explains why the magnetodispersion curve of the axisymmetric plasmon mode is parabolic [Fig. 1(b)].

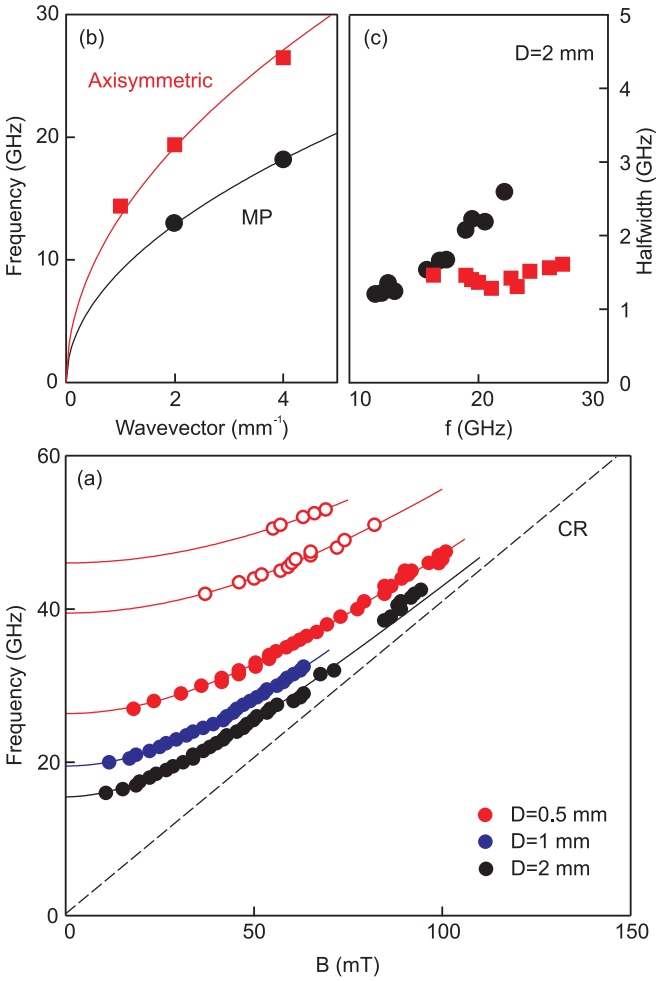

FIG. 2. (a) Magnetodispersion curves of dark axisymmetric plasma modes for quasi-Corbino samples with different mesa diameters $D = 2, 1, 0.5$ mm. Empty circles denote multiple harmonics of the fundamental magnetoplasmon resonance for the sample with $D = 0.5$ mm. The electron density in all samples is $n_s = 1.0 \times 10^{11}\text{cm}^{-2}$. (b) Comparison of the dispersions of axisymmetric (squares) and fundamental (circles) plasmon modes. Solid lines correspond to a square-root fit to the experimental points. (c) Mode linewidth versus resonance frequency for the axisymmetric (squares) and fundamental (circles) plasmon modes.

Since the most important characteristic of plasma excitation is its dispersion, the experiment outlined above was repeated for a set of samples with outer diameters, $D = 2, 1$, and 0.5 mm in order to understand the dispersion properties of axisymmetric plasma waves involved in our investigation. The corresponding magnetodispersion dependencies are plotted in Fig. 2(a). A fit of the experimental data with Eq. (3) yielded the following zero-field plasma frequencies: $f_0(D = 2\,\text{mm}) = 14.4\,\text{GHz}$, $f_0(D = 1\,\text{mm}) = 19.4\,\text{GHz}$, and $f_0(D = 0.5\,\text{mm}) = 26.5$ GHz. We then assigned a corresponding wave vector $q = 2/D$ [7], to each of these three modes, and plotted the experimentally obtained dispersion points for the axisymmetric dark plasma excitations [Fig. 2(b), squares]. For comparison, the dispersion of the fundamental bright 2D plasma modes $(m = 1; l = 1)$ observed in a single disk is shown in the same plot for the same electron density [Fig. 2(b), circles]. The experimental points for the fundamental plasma excitation perfectly follow the standard square-root dispersion law as prescribed by Eq. (1) [Fig. 2(b), solid black line] [7,9]. The dispersion of the axisymmetric plasmon was found to follow the square-root law [as depicted by the solid red line in Fig. 2(b)], but with a frequency $K = (1.5 \pm 0.1)$ times larger frequency than the fundamental mode frequency. This finding agrees qualitatively with the theoretical prediction [7]. However, the theory yields the coefficient value of $K = 1.86$. This deviation between experiment and theory likely stems from the fact that the hydrodynamic model [7] poorly describes the dynamics of unscreened 2D electron plasma, inherently present in our experiments.

The most important characteristic of plasma waves in applications is their damping rate. Plasmon resonance width is determined by the sum of the incoherent collisional damping term, $\gamma = 1/\tau$, which is given by the characteristic scattering time τ, and the coherent superradiant damping contribution Γ, $\Delta\omega = \gamma + \Gamma$ [20–24]. The superradiant contribution arises from the dipole reradiation of electromagnetic waves generated by coherently oscillating 2D electrons, and in many cases, it is these high radiative losses that act as the primary factor inhibiting the excitation of plasma waves in 2DESs [25,26].

The most distinctive feature of axisymmetric dark plasma excitations is their zero total dipole moment. This symmetry property suppresses superradiant losses, leading to significantly longer lifetimes. In order to verify this phenomenon, we measured the mode linewidth versus the frequency for axisymmetric dark (squares) and fundamental bright (circles) plasma excitations [Fig. 2(c)]. Our experiments were performed on samples of identical size, $D = 2$ mm, and electron density $n_s = 1.0 \times 10^{11}\text{cm}^{-2}$. The half-width of the resonance Δf was calculated by multiplying the half-width ΔB on the magnetic field by the slope of the magnetodispersion curve, evaluated at the field at which the resonance occurred: $\Delta f = (\partial f/\partial B)\Delta B$. We see from Fig. 2(c) that the bright plasmon mode width (circles) saturates at a constant level of $\gamma/2\pi \approx 1$ GHz in the low frequency limit. However, as the magnetoplasmon frequency is increased, the mode width rises rapidly due to the superradiant decay from the coherent dipole reradiation generated by oscillating 2D electrons [23,24]. In contrast, the dark plasmon width (squares) stays at a constant level $\gamma/2\pi \approx 1$ GHz across the entire experimental frequency range, and exhibits no contribution from the superradiant losses.

In summary, we demonstrated the excitation of axisymmetric dark plasmon modes in semiconductor nanostructures using a two-dimensional electron system of special geometry. The observed modes exhibit very peculiar physical properties, and in particular, we experimentally demonstrated a strong suppression of superradiant losses in these collective plasmon excitations, originating from their zero dipole moments. This desirable feature results in much narrower plasmon resonance linewidths making these modes highly attractive for creating high-quality plasmonic devices.

The authors gratefully acknowledge financial support from the Russian Science Foundation (Grant No. 14-12-00599).

[1] J. Łusakowski, Semicond. Sci. Technol. **32**, 013004 (2016).
[2] W. Knap, Y. Deng, S. Rumyantsev, and M. S. Shur, Appl. Phys. Lett. **81**, 4637 (2002).
[3] X. G. Peralta, S. J. Allen, M. C. Wanke, N. E. Harff, J. A. Simmons, M. P. Lilly, J. L. Reno, P. J. Burke, and J. P. Eisenstein, Appl. Phys. Lett. **81**, 1627 (2002).
[4] E. A. Shaner, M. Lee, M. C. Wanke, A. D. Grine, J. L. Reno, and S. J. Allen, Appl. Phys. Lett. **87**, 193507 (2005).
[5] V. M. Muravev and I. V. Kukushkin, Appl. Phys. Lett. **100**, 082102 (2012).
[6] F.-P. Schmidt, H. Ditlbacher, U. Hohenester, A. Hohenau, F. Hofer, and J. R. Krenn, Nat. Commun. **5**, 3604 (2014).
[7] A. L. Fetter, Phys. Rev. B **33**, 5221 (1986).
[8] S. J. Allen, H. L. Störmer, and J. C. M. Hwang, Phys. Rev. B **28**, 4875 (1983).
[9] F. Stern, Phys. Rev. Lett. **18**, 546 (1967).
[10] I. V. Kukushkin, J. H. Smet, S. A. Mikhailov, D. V. Kulakovskii, K. von Klitzing, and W. Wegscheider, Phys. Rev. Lett. **90**, 156801 (2003).
[11] D. C. Glattli, E. Y. Andrei, G. Deville, J. Poitrenaud, and F. I. B. Williams, Phys. Rev. Lett. **54**, 1710 (1985).
[12] D. B. Mast, A. J. Dahm, and A. L. Fetter, Phys. Rev. Lett. **54**, 1706 (1985).
[13] B. M. Ashkinadze, E. Linder, E. Cohen, and A. Ron, Phys. Status Solidi A **164**, 231 (1997).
[14] I. V. Kukushkin, J. H. Smet, K. von Klitzing, and W. Wegscheider, Nature (London) **415**, 409 (2002).
[15] S. S. Nazin and V. B. Shikin, Fiz. Nizk. Temp. **15**, 227 (1989) [Sov. J. Low Temp. Phys. **15**, 127 (1989)].
[16] A. V. Chaplik, Zh. Eksp. Teor. Fiz. **62**, 746 (1972) [Sov. Phys. JETP **35**, 395 (1972)].
[17] T. N. Theis, J. P. Kotthaus, and P. J. Stiles, Solid State Commun. **24**, 273 (1977).
[18] T. Demel, D. Heitmann, P. Grambow, and K. Ploog, Phys. Rev. B **38**, 12732(R) (1988).
[19] E. Vasiliadou, G. Müller, D. Heitmann, D. Weiss, K. von Klitzing, H. Nickel, W. Schlapp, and R. Lösch, Phys. Rev. B **48**, 17145 (1993).
[20] I. V. Andreev, V. M. Muravev, V. N. Belyanin, and I. V. Kukushkin, Appl. Phys. Lett. **105**, 202106 (2014).
[21] Qi Zhang, T. Arikawa, E. Kato, J. L. Reno, W. Pan, J. D. Watson, M. J. Manfra, M. A. Zudov, M. Tokman, M. Erukhimova, A. Belyanin, and J. Kono, Phys. Rev. Lett. **113**, 047601 (2014).
[22] T. Laurent, Y. Todorov, A. Vasanelli, A. Delteil, C. Sirtori, I. Sagnes, and G. Beaudoin, Phys. Rev. Lett. **115**, 187402 (2015).
[23] V. M. Muravev, I. V. Andreev, S. I. Gubarev, V. N. Belyanin, and I. V. Kukushkin, Phys. Rev. B **93**, 041110(R) (2016).
[24] I. V. Andreev, V. M. Muravev, V. N. Belyanin, S. I. Gubarev, and I. V. Kukushkin, Pis'ma Zh. Eksp. Teor. Fiz. **102**, 938 (2015) [JETP Lett. **102**, 821 (2015)].
[25] R. H. Dicke, Phys. Rev. **93**, 99 (1954).
[26] S. A. Mikhailov, Phys. Rev. B **54**, 10335 (1996).